A novel electrocatalyst support with proton conductive properties for polymer electrolyte membrane fuel cell applications

Marcelo Carmo [a,b,*], Thorsten Roepke [c], Christina Roth [d],
Amilton M. dos Santos [e], Joao G.R. Poco [b], Marcelo Linardi [a]

[a] Nuclear and Energetic Research Institute – IPEN, Av. Prof. Lineu Prestes 2242, Cidade Universitária, 05508-000, Sao Paulo, Brazil
[b] Technological Research Institute - IPT, Av. Prof. Almeida Prado 532, Cidade Universitaria, 05508-901, Sao Paulo, Brazil
[c] Hydrogen Institute of Applied Technologies – HIAT, Hagenower Straße 73, D-19061 Schwerin, Germany
[d] Technische Universität Darmstadt – TUD, Petersstrasse 23, D-64287 Darmstadt, Germany
[e] University of São Paulo – USP, Estrada Municipal do Campinho, S/N, 12602-810, Lorena (SP), Brazil

ARTICLE INFO

ABSTRACT

The objective of this study is to graft the surface of carbon black, by chemically introducing polymeric chains (Nafion® like) with proton-conducting properties. This procedure aims for a better interaction of the proton-conducting phase with the metallic catalyst particles, as well as hinders posterior support particle agglomeration. Also loss of active surface can be prevented. The proton conduction between the active electrocatalyst site and the Nafion® ionomer membrane should be enhanced, thus diminishing the ohmic drop in the polymer electrolyte membrane fuel cell (PEMFC). PtRu nanoparticles were supported on different carbon materials by the impregnation method and direct reduction with ethylene glycol and characterized using amongst others FTIR, XRD and TEM. The screen printing technique was used to produce membrane electrode assemblies (MEA) for single cell tests in H_2/air (PEMFC) and methanol operation (DMFC). In the PEMFC experiments, PtRu supported on grafted carbon shows $550\,mW\,cm^{-2}\,gmetal^{-1}$ power density, which represents at least 78% improvement in performance, compared to the power density of commercial PtRu/C ETEK. The DMFC results of the grafted electrocatalyst achieve around 100% improvement. The polarization curves results clearly show that the main cause of the observed effect is the reduction in ohmic drop, caused by the grafted polymer.

1. Introduction

Carbon black has been frequently used as a catalyst support in polymer electrolyte membrane fuel cells (PEMFCs), because of its stability in both acid and basic media, good electronic conductivity and high specific surface area. The support material has a strong influence on the properties of the catalysts, such as metal particle size, electrochemical active area and size distribution. Furthermore, degree of alloying, stability, mass transport and electronic conductivity of the catalyst layer are also affected by the chosen support material. Hence, the development of novel carbon supports plays an important role for the future PEMFC technology. The support should be properly selected, with a suitable specific surface area, porosity, morphology, surface functional groups and electronic conductivity. Corrosion resistance is also a crucial parameter to be considered, while developing an active commercial catalyst. Most of these parameters are affected by the process used to prepare the carbon black. Some parameters such as, surface area, which is accessible and sufficiently large for maximum catalyst dispersion, pore size, pore distribution and surface functional groups of carbon blacks are being discussed as essential for optimized carbon supports. These parameters also affect the preparation and performance of carbon black used in a fuel cell electrode. Carbon black still reveals inadequacies for this purpose [1,2]. For example, in a conventional impregnation process, some of the metal nanoparticles could sink into the micropores of carbon black or strongly attach to its impurities. The electrochemical activity could be reduced or hindered due to reactant inaccessibility to the metal nanoparticles inside the micropores or adsorbed at the impurities. This is the main reason, why some catalysts prepared by the impregnation method have not shown high activities even when the metal loading was very high.

In the electrocatalysis process, in a polymer electrolyte membrane fuel cell, operating with H_2/O_2, the hydrogen molecules must be first distributed in the porous gas diffusion electrode and they rapidly reach the nanoparticulate metal surfaces, providing the cat-

* Corresponding author at: Nuclear and Energetic Research Institute – IPEN, Av. Prof. Lineu Prestes 2242, Cidade Universitária, 05508-000, Sao Paulo, Brazil. Tel.: +55 11 37674619.
E-mail address: mcarmo@ipt.br (M. Carmo).

alytic active sites. The species must electrochemically adsorb on the metal and be oxidized, releasing thereby an electron to the metal and to the carbon particles, which finally enters the external circuit. The protons formed in this process have to be transported from the catalytic site to the electrolyte membrane, mostly Nafion®, then cross the membrane and react with the O_2 molecule at the cathode side to produce H_2O as a final product. To get a more efficient H^+ conduction from the catalytic site to the membrane, a certain amount of dispersed Nafion® ionomer in the porous gas diffusion electrode is usually used to enhance platinum utilization.

The contact between the metal nanoparticles and the Nafion® ionomer micelles in the catalytic layer of the gas diffusion electrode is crucial and is also affected by the carbon pore size and its distribution. As reported by Uchida et al. [3], the Nafion® ionomer has micelles of about 40 nm in size. The nanoparticles, which sink into the carbon pores with diameters below 40 nm, have no access to the Nafion® ionomer and thus do not contribute to the total catalytic activity. Consequently, catalytic utilization of the metal nanoparticles is determined by electrochemical accessibility and not by the carbon surface area. Recently, Rao et al. [4] have investigated the effect of carbon porosity on PtRu/C specific activity for methanol oxidation. They have found that for carbon black with a large concentration of small diameter pores (<20 nm), which were filled with metal nanoparticles, the contact between the Nafion® micelles and the metal nanoparticles was very poor, resulting in a low methanol oxidation activity. These authors have reported that 20% of PtRu supported on a specific Sibunit carbon black (Sib-19P; $S_{BET} = 72\ m^2\ g^{-1}$) showed an activity of 180 mA mgmetal^{-1} at 500 mV in a half cell test (DMFC). This performance was six times higher compared to another Sibunit carbon (PtRu/Sib-619P; $S_{BET} = 415\ m^2\ g^{-1}$). Hence these authors have concluded that an increase in the carbon surface area did not increase the catalytic activity.

On the basis of these facts, three distinct interfaces have been identified, which are responsible for improving or deteriorating the catalytic performance of a PEMFC: (1) metal–C interface, (2) metal–Nafion® interface and (3) C–Nafion® interface. Consequently, the development of electrocatalysts with improved performance for H_2 oxidation as well as for methanol oxidation has to search for new materials with optimized physical and chemical conditions at these interfaces. One approach would be the chemical modification of the surface of the carbon black support used to anchor the nanoparticles of the electrocatalysts. In this case, the modifications at the micro(nano)scopic level could be done by linking simple organic compounds and eventually growing macromolecules. Chemical reactions could be applied to encapsulate, protect and change the hydrophobic/hydrophilic character of the materials. By this means, the reactivity can be changed, catalytic properties modified as well as composites created and polarities changed (zeta potential) [5–8].

The grafting of polymers onto and from carbon black surfaces has been widely investigated. There are two ways to attach polymers to carbon materials; *graft-onto* and *graft-from*. Graft-onto requires the attachment of separately prepared polymer to carbon black and graft-from involves the growth of the desired polymer directly from the carbon surface using previously attached initiators, via several polymerization intermediates [9–11]. In general, polymer is grafted onto the surface during polymerization in the presence of carbon black, but the percentage of grafting is very low. It is well known that carbon black itself has unpaired electrons [12], but these unpaired electrons have no ability to initiate the radical polymerization of vinyl monomers, because the unpaired electrons are stabilized by the polycondensed aromatic rings of carbon black and therefore the introduction of active radical groups onto the carbon black surface is required. To prepare the polymer grafted carbon black with a higher percentage of grafting, it is necessary to initiate the graft polymer-

ization from active sites on the carbon black surface [13]. There are other ways to get carbon black grafted. For example: using radical [14,15], anionic [16] or cationic [17] initiators, by cationic grafting from acylium perchlorate groups on carbon black [13,18], by graft polymerization from carbon black initiated with a redox system, consisting of ceric ions and alcoholic hydroxyl groups introduced onto the surface [19] and by reacting azo groups onto the carbon black surface [20].

The objective of this study is the cationic grafting of styrene sulphonic from carbon black surface, followed by the physical, chemical and electrochemical characterization of the carbon support. The characterization of PtRu electrocatalysts supported on the new grafted material for PEMFC and DMFC applications is also performed.

2. Experimental

2.1. Grafting of poly(styrene sulphonic) from carbon black surface [21]

2.1.1. Introduction of carboxyl groups onto carbon black

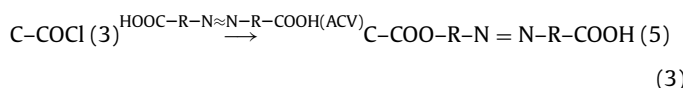$$C\ (1) \xrightarrow{HNO_3} C\text{–}COOH\ (2) \tag{1}$$

The introduction of carboxyl groups onto carbon black (2) was achieved by treatment of carbon black (1) with nitric acid. Into a glass thermostatized reactor, 15 g of carbon black and 300 mL of concentrated nitric acid were charged. The mixture was stirred for 24 h at 80 °C. The resulting carbon was filtered, thoroughly washed with Milli-Q water until nitrate removal and dried with air in an oven at 110 °C for 2 h. The sample was labeled C–COOH.

2.1.2. Introduction of acyl chloride groups onto carbon black

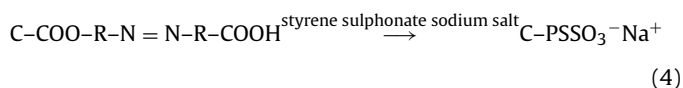$$C\text{–}COOH\ (2) \xrightarrow{SOCl_2} C\text{–}COCl\ (3) \tag{2}$$

Carbon black having acyl chloride groups (3) was prepared by the reaction of carboxylic functionalized carbon black (2) with thionyl chloride. Carbon black (5 g) was charged in 50 mL of absolute benzene. A large excess (15 mL) of $SOCl_2$ was added and the mixture was stirred and refluxed for 50 h. After the reaction, benzene and unreacted $SOCl_2$ were distilled under reduced pressure and then the resulting carbon black was dried at 110 °C in vacuum. The treated carbon black was stored in vacuum in the dark. The sample was labeled C–COCl.

2.1.3. Introduction of azo groups onto carbon black

$$C\text{–}COCl\ (3) \xrightarrow{HOOC\text{–}R\text{–}N \approx N\text{–}R\text{–}COOH(ACV)} C\text{–}COO\text{–}R\text{–}N = N\text{–}R\text{–}COOH\ (5) \tag{3}$$

To a pre-dissolved 4,4′-azobis(4-cyanovaleric acid) (4) (500 mg) in 60 mL chloroform, 500 mg of carbon black with acyl chloride groups (3) was added and the mixture was stirred for 24 h at 25 °C. After the reaction, the resulting carbon black (5) was filtered and repeatedly washed with chloroform and dried in vacuum at room temperature. The treated carbon black was stored in the dark below 0 °C. The sample was labeled C-azo.

2.1.4. Polymerization of styrene sulphonic sodium salt monomer from carbon black surface

$$C\text{–}COO\text{–}R\text{–}N = N\text{–}R\text{–}COOH \xrightarrow{styrene\ sulphonate\ sodium\ salt} C\text{–}PSSO_3{}^-Na^+ \tag{4}$$

$$C\text{–}PSSO_3{}^-Na^+ \xrightarrow{H_2SO_4} C\text{–}PSSO_3{}^-H^+ \tag{5}$$

To pre-dissolved styrene sulphonic sodium salt monomer (1.5 g) in 100 mL Milli-Q H_2O, 500 mg of carbon black with azo groups was added and the mixture was stirred for 1 h at 80 °C (4). After the reaction, 100 mL of sulfuric acid 0.5 mol L^{-1} was added and mechanically stirred for 1 h at 80 °C in order to change the cation in the sulfuric group of the polymer, from Na^+ to H^+, to make the polymer proton conductive (5). The resulting carbon black was filtered and repeatedly washed with water and dried at 100 °C. The final product was labeled C-PSSH.

2.2. Preparation of electrocatalysts

The carbon-supported electrocatalysts were prepared using the impregnation method and subsequent reduction with an alcohol. A mixture of the desirable metallic ions in solution was used as precursor. The ions in the solution were reduced to their metallic form, using ethylene glycol (Merck) as solvent and a reducing agent in the presence of the carbon support. PtRu/C (20 wt.%, Pt:Ru atomic ratio of 1:1) was prepared using this procedure. $H_2PtCl_6 \cdot 6H_2O$ (Aldrich) and $RuCl_3 \cdot 2H_2O$ (Aldrich) were used as metal sources.

High surface area carbon black Vulcan XC-72 in the as-received condition and grafted carbon black Vulcan XC-72 was used as supports. In this procedure the salts were first added to the carbon support, followed by an ethylene glycol solution (75:25, ethylene glycol:water). The system was ultrasonically treated for 15 min. It was then refluxed and heated at 160 °C for 1 h. The resulting powder was filtered, washed and dried overnight at 110 °C. Commercial electrocatalysts PtRu/C (20 wt.%, Pt:Ru atomic ratio of 1:1) from ETEK and HISPEC were used for comparison.

2.3. Characterization of physical properties

2.3.1. Potentiometric titration

The titration method was used to determine the quantity of H^+ and consequently, the quantity of polymers grafted on the carbon surface. The potentiometric titration method was performed using standard NaOH that had previously been degassed with N_2 and the carbon grafted material to be titrated was previously stirred in CO_2 degassed Milli-Q H_2O for 24 h. During data acquisition, each curve point was registered after 1 h of stabilization.

2.3.2. Infra red spectrometry analysis

The infra red spectra were registered on a Nicolet FTIR-8100 spectrometer in KBr matrix. The KBr was previously heat treated at 400 °C for 2 h in air and was kept inside a dessiccator with $CaCl_2$.

2.3.3. Brunauer–Emmet–Teller (BET) surface area analysis

A NOVA 300 BET (Brunauer–Emmet–Teller) Analyzer was used to determine the specific surface area of the carbons. Prior to measurement, the carbon samples were purged with pure nitrogen gas overnight at 150 °C to remove contaminants and moisture that could be in the carbons.

2.3.4. Laser scattering (LS) analysis

A Laser Scattering LS230 Small Volume Module Plus – Coulter was used to estimate the average particle size of the carbons. Before measurement, 5 mg of the sample was dispersed in water and ultrasonically dispersed for at least 48 h.

2.3.5. Thermogravimetric analysis (TGA)

A Thermal Analysis System STAR TGA/SDTA851^e Module from Mettler Toledo with Star-e version SW 8.01 software was used for thermo gravimetric analysis. A heating rate of 10 °C min^{-1} and a nitrogen flux of 50 mL min^{-1} were used.

2.3.6. EDX and X-ray diffraction (XRD)

The Pt:Ru atomic ratios of the electrocatalysts were obtained by using a Philips XL30 scanning electron microscope coupled to an EDAX DX-4 microanalyzer with a 20 keV electron beam. The X-ray diffraction analyses were performed using a STOE STADI-P diffractometer with germanium monochromized Cu Kα radiation and position-sensitive detector with 40 aperture in transmission mode. The X-ray diffractograms were obtained with a scan rate of 1 min^{-1} and an incident wavelength of 1.5406 Å (Cu Kα). The average crystallite size was estimated using the XRD data and the Scherrer equation.

2.3.7. Transmission electron microscopy (TEM)

The transmission electron microscopy characterization was done using a JEOL JEM-1200EX microscope and the average particle size was calculated using the Image Tool Software with one TEM micrograph for each catalyst.

2.3.8. Electrochemical characterization

To prepare the MEA's, water and a desired amount of the conducting polymer solution (Nafion®) were added to the catalyst powder. The system was emulsified with a ultra-turrax system for 10 min and stirred at 90 °C, until the loss of water was sufficient, resulting in an optimum paste to be applied by the sieve printing technique. The amount of catalytic material (metal loading) was controlled after the printing process. After sieve printing, heat treatment was carried out at 135 °C for 30 min. The membrane was treated with 5 wt.% nitric acid at 100 °C and then washed in hot Milli-Q water, followed by cold Milli-Q water. The MEA were placed in the single cell, using as gas diffusion layer Toray paper (TGP-H-060) in the anode and Sigracet 10CC in the cathode. The experimental conditions for PEMFC were test cell: HIAT FC25/125; contact pressure on electrochemically active area: 1 N mm^{-2}; cathode—air: 1.5 NL min^{-1} (100% humidity); anode—H_2 0.8 mL min^{-1}; cell temperature: 70 °C; GDLs: anode Toray TGP-H-060; cathode Sigracet 10CC. The experimental conditions for DMFC were test cell: HIAT FC25/125; contact pressure on electrochemically active area: 1 N mm^{-2}; air: 1.5 NL min^{-1} (100% humidity); CH_3OH 3.5%: 15 mL min^{-1}; cell temperature 70 °C; GDLs: anode – 0.6 mg_{PtRu} cm^{-2}, Toray paper TGP-H-060; cathode – 1.5 mg_{Pt} cm^{-2}, Toray paper Sigracet 10CC; Nafion® membrane 117.

3. Results

3.1. Physico-chemical characterization of the polystyrene sulphonic grafted carbon black

3.1.1. Fourier transform infra red (FTIR) spectroscopy

Fig. 1 presents the infrared spectroscopy results of commercial carbon black, carbon black after functionalization with HNO_3, after $SOCl_2$ funcionalization, after azo agent functionalization and the carbon black grafted with polystyrene sulphonic. Fig. 1 presents also the infrared spectroscopy results for the azo agent. Fig. 2 compares the grafted carbon black, the pure polystyrene sulphonic polymer, the styrene sulphonic sodium salt monomer and the commercial Nafion® membrane. The wavelenght and the intensity of the characteristic absorption bands of the functional groups in the respective spectra is compared. In sample 1, carbon black functionalized with nitric acid (shown in the spectra in Fig. 1), the peaks in the region of 1860–1650 cm^{-1} (1) are attributed to the stretching of C=O related to the cabonyl and carboxyl groups [22]. The spectra also shows peaks at 1740 cm^{-1} (2), that could be associated to the lactones groups [22]. Data [23] are available in literature about C=O streching/vibration from carboxylic groups near aromatic rings and these generally present peaks between 1700 and 1680 cm^{-1}. The wave number is affected by the different periperic groups [23]. The peak
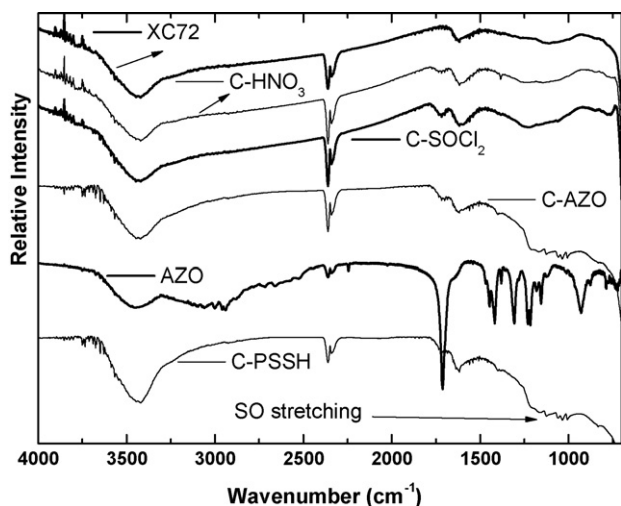
Fig. 1. FTIR spectra for Vulcan XC-72, C-HNO₃, C-SOCl₂, C-AZO e C-PSSH.

Table 1
BET surface area and LS particle size results.

	Surface area ($m^2 g^{-1}$)	Particle size (μm)
Vulcan XC-72	232	14.9
Vulcan XC-72-PSSH	39	0.06

face. FTIR spectroscopy is probably not sensitive enough to detect the chloride groups in these carbon samples. For sample 3, carbon black functionalized with the ACPA based (ou derived) azo component (ou coupling agent) groups (shown in Fig. 1), the peaks at 1500–1200 cm^{-1} can be attributed to the azo groups strechings on the carbon surface. For sample 4, grafted carbon black with polystyrene sulphonic, peaks in the region at 1200–1000 cm^{-1} (8), in Fig. 1, can be attributed to the sulphonic groups stretching. In Fig. 2, the same peaks related to the sulphonic groups in all samples can be seen. Qualitatively, the FTIR spectroscopy revealed that the synthesis route to graft carbon black was very successful.

at 1580 cm^{-1} (3), that appears in the original sample and in the HNO₃ oxidized sample has been observed by many authors and associated to the aromatic ring streching, coupled to the carbonyl group and moreover, to the increase in the C=O bond streching [22]. The peak at 1460 cm^{-1} (4), could be associated to O–H vibration deformation in the carboxylic groups and also to the C–H vibrations [22–25]. The peaks in the region between 1400 and 1380 cm^{-1} (5) can be attributed to carboxyl-carbonate structure [5,22] or to the aromatic bond C=C and also to several aromatic ring substitutions [22]. Peaks between 1200 and 1000 cm^{-1} (6) are difficult to identify, because of the large number of overlapping peaks and therefore cannot be attributed to functional groups or chemical bonds [22]. Peaks below 950 cm^{-1} (7) are characteristic of vibration deformation of the C–H group plane in the aromatic structures [5,22,26]. Gomezserrano et al. [27] have also showed the presence of N–O and –NO₂ groups that take the place of hydrogen in the carbon structure. Salame and Bandosz [28] have also discussed the presence of peaks related to nitrogenated groups between 1540 and 1350 cm^{-1}. Barkauskas and Dervinyte [29] have reported that by carbon functionalized with nitric acid, the carboxylic groups is introduced to greater extent and phenols and lactones groups to lesser extent. For sample 2, carbon black functionalized by thionyl chloride (shown in the spectra of Fig. 1), there is no information about the incorporation of chloride groups in the carbon black sur-
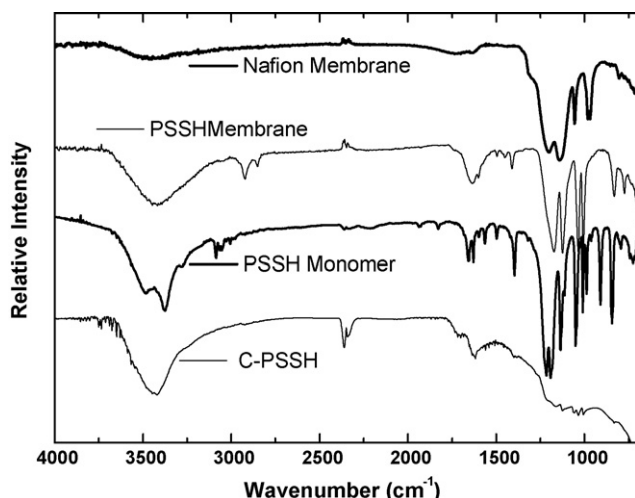
3.1.2. Brunauer–Emmet–Teller (BET) surface area results

Table 1 shows the specific surface area results of the carbons. After grafting, it can be seen that the surface area of the carbon is reduced by 85%, which indicates that the treatment caused changes in the carbon structure. Chen and Wu [30] have showed a slight reduction in the surface area of carbons, after dilute HNO₃ treatment and have showed also that organic acids with higher molecular size could better penetrate the carbon structure, resulting in pore blockage. This behavior was also noted by Gomezserrano et al. [27]. As indicated in the literature [24,31–33], oxidation treatments produce a large amount of oxygenated groups (carboxylic, hydroxyl, lactones, etc.) on the carbon surface. These groups are responsible for changing not only the acid-basic character of the carbon black, but also the pore structure. The pore structure of carbon black is of great importance in the development of support material for DMFC applications, as discussed in Section 1. Carbon micropores filled with metal catalysts are undesirable as they restrict the access of the reactants to the active sites, resulting in waste of noble catalysts. It has been suggested that the oxygen surface groups are fixed at the entrance of micropores after carbon functionalization. This effect is much more evidenced for the grafted carbon with polymeric chains. In this case, the polymeric chains block the diffusion of species into the carbon micropores. Some authors [24,31–33] have reported similar restrictions for diffusion in micropores of carbon black after other chemical treatment. In this study, the blocking of micropores can be clearly seen from the BET results. The model of the carbon pore structure, before and after the grafting, is shown in Fig. 3.

3.1.3. Laser scattering results

Table 1 shows the carbon particle size average in water media, as determined with a laser scattering technique. A reduction in the average particle size of carbon black can be seen. After grafting, the carbon black became much more hydrophilic and consequently, the dispersion of the carbon black in water is facilitated. The particle size of grafted carbon black dispersed in water is significantly smaller than the carbon black without grafting, thus indicating a beneficial behavior in terms of electrocatalyst preparation, as well as for the final MEA preparation, using electrocatalyst inks (Fig. 4). As shown in Fig. 5, a much more carbon particle stabilized dispersion (in water) is obtained after grafting. The system was placed for decantation for 5 months and no obvious sedimentation is observed.

3.1.4. Thermogravimetric analysis results

The relative content of polystyrene sulphonic grafted carbon black compared to commercial carbon black was determined from thermogravimetric analysis and is shown in Fig. 6. The grafted car-
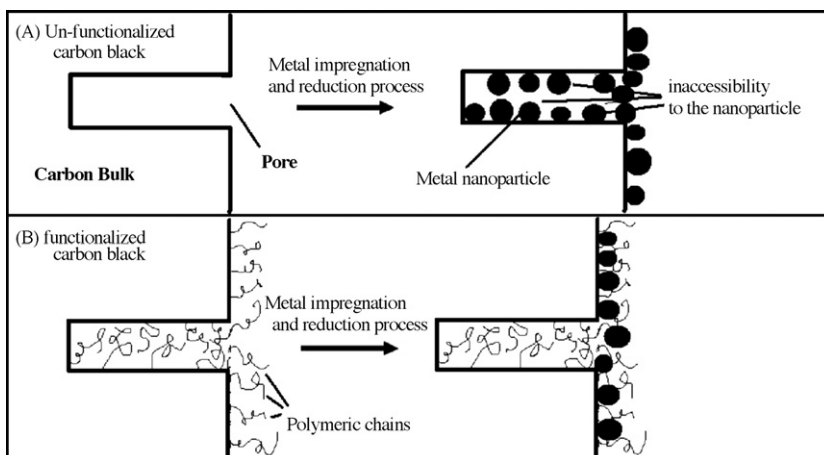

Fig. 2. FTIR spectra for C-PSSH and polystyrene sulphonic.

Fig. 3. Model of the carbon pore blockage before and after the grafting.
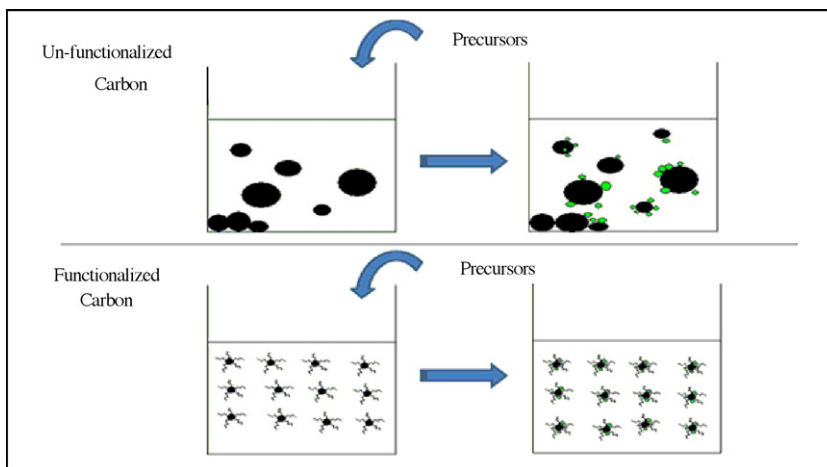

Fig. 4. Model of the grafted carbon black stabilization in water media, in the PEM fuel cell electrocatalysts preparation.

bon black shows a gradual mass loss of about 10% from 25 to 110 °C, mainly loss of water. The presence of water in the grafted carbon black can be attributed to its hydrophilic nature. In the range 150–1000 °C the polymer decomposed and the content of polymer grafted from the carbon black was 20%, as intended. In Fig. 7, at 140 °C the melting point of polymer in the grafted carbon black surface can be observed.

3.2. Physico-chemical characterization of the PtRu electrocatalyst supported on poly(styrene sulphonic) grafted carbon black.

3.2.1. Energy dispersive analysis of X-rays (EDX), X-ray diffraction analysis and transmission electron microscopy results

The Pt:Ru atomic ratios of the electrocatalysts, which were determined by EDX, are very close to the nominal composition, calculated from the mass of the metallic components, which were used. All the
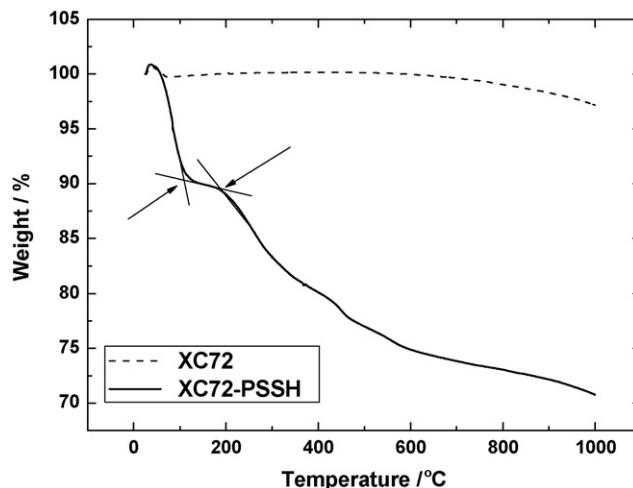

Fig. 5. Solubility photo of carbon black (left) and grafted carbon black (right) in water.

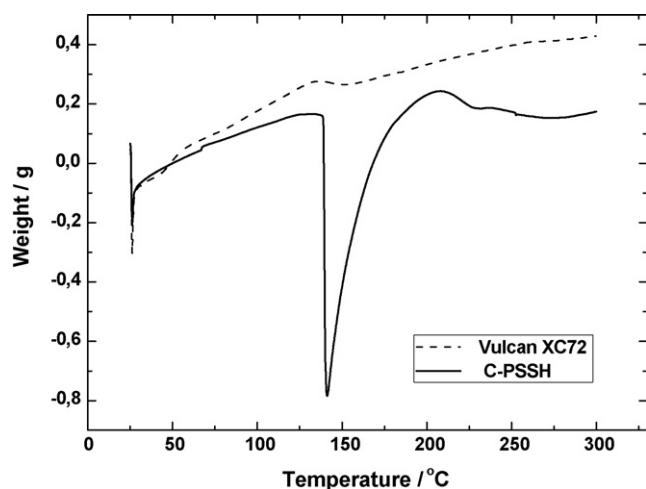**Fig. 6.** TGA curves of carbon black and polystyrene sulphonic grafted carbon black.

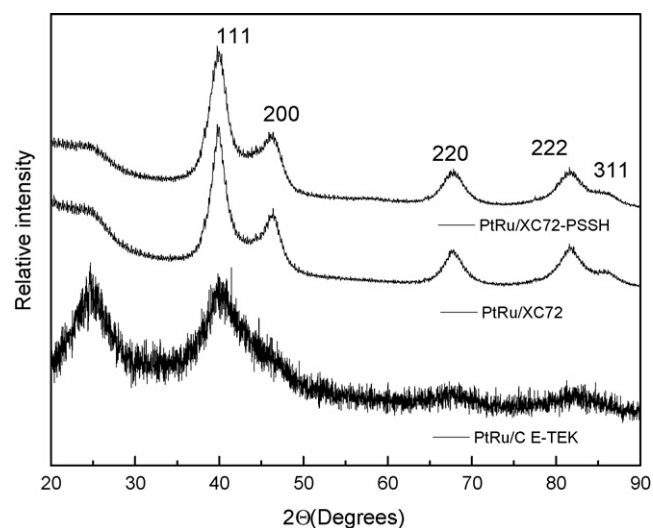Fig. 7. DSC curve of polystyrene sulphonic grafted carbon black.

Fig. 8. X-ray diffractograms for the PtRu/C supported electrocatalysts.

electrocatalysts show diffraction peaks at about $2\theta = 40°$, $47°$, $67°$ and $82°$ (Fig. 8), characteristic of the FCC structure of platinum and platinum alloys [34–36]. The broad peak at about $2\theta = 25°$ is associated with the carbon black used as support material, as discussed before. For the PtRu/C electrocatalysts, no other peaks of the HCP phase of ruthenium or ruthenium oxides are observed. The average

particle size, L, can be estimated from the Scherrer equation, Eq. (6), using the platinum peak (2 2 0) [36]:

$$L = \frac{0.9\lambda_{k_{\alpha 1}}}{B_{(2\theta)} \cos \theta_{\max}} \tag{6}$$

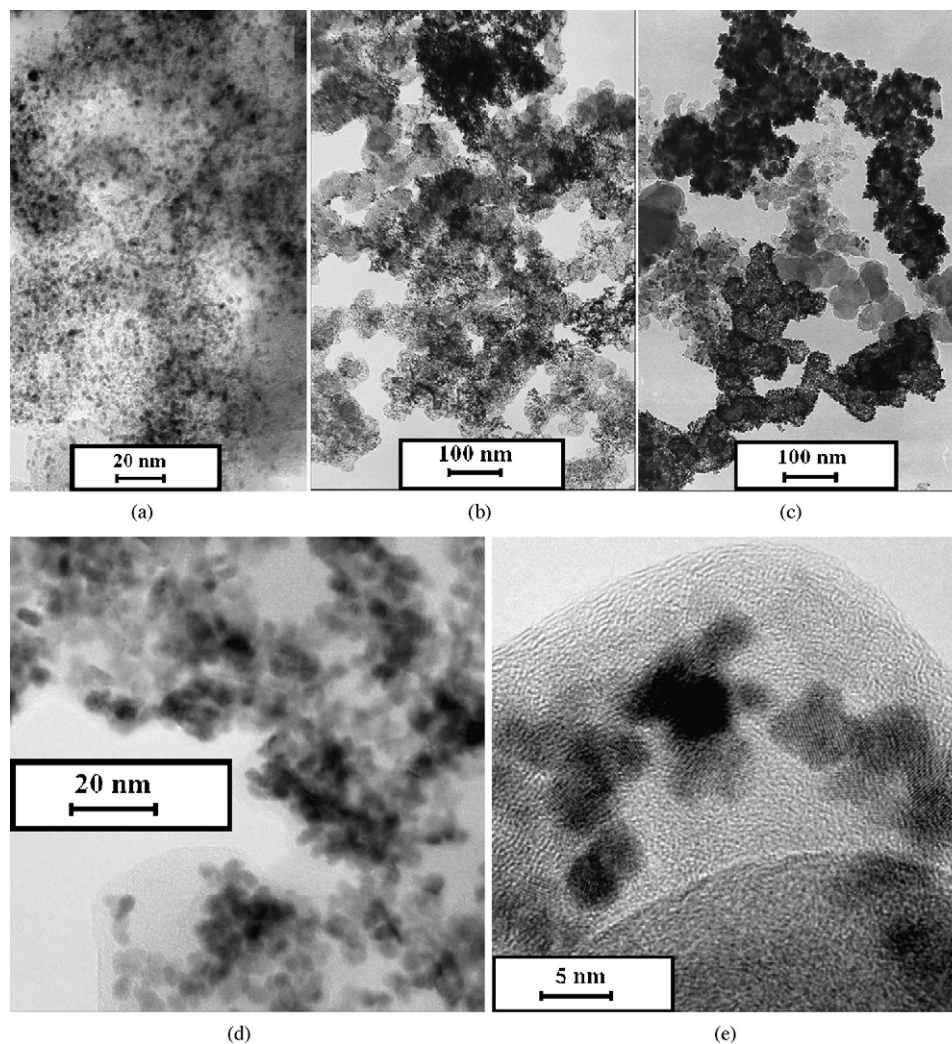(a)   (b)   (c)

(d)   (e)

Fig. 9. TEM micrographs for (a) PtRu/C ETEK, (b) PtRu/C HISPEC, (c) PtRu/C, (d) PtRu/C-PSSH and (e) PtRu/C-PSSH (another sample).

Table 2
XRD and TEM particle size results for the PtRu/C electrocatalysts.

	Diameter (nm) XRD	Diameter (nm) TEM
PtRu/C-PSSH	3.7	3.2
PtRu/C	4.3	4.7
PtRu/C ETEK	<2	2.8
PtRu/C Hispec	–	3.9

where $\lambda_{k_{\alpha 1}}$: wavelength, $\lambda_{k_{\alpha 1}}$ is 1.54056 Å and the full-width half-maximum $B_{(2\Theta)}$ is in radians.

The XRD results show that alcohol reduction produces nanoparticles in the desirable size range for fuel cell applications (Table 2).

The PtRu/C catalyst from ETEK has a smaller crystallite size compared to the PtRu/C catalyst. However the crystallite size of the polymer grafted carbon is smaller than that of the ungrafted carbon.

The TEM images in Fig. 9a–e reveal a very homogenous and uniform particle distribution for PtRu/ETEK (Fig. 9a) and for PtRu/C with grafted polymer (Fig. 9d). The materials PtRu/C HISPEC (Fig. 9b) and PtRu/C without treatment (Fig. 9c) reveal many agglomerates and a non-uniform particle distribution.

3.3. Fuel cell operation results

The PEMFC polarization curves and power density curves, working with hydrogen and air, are shown in Fig. 10. The cathode was set as standard, using commercially available Pt/C HISPEC and Pt/C ETEK electrocatalysts. The PtRu/C-PSSH achieves a maximum power density of 535 mW cm^{-2} gmetal^{-1}. The PtRu/C catalyst without treatment achieves 305 mW cm^{-2} gmetal^{-1}. The PtRu/C ETEK achieves 35 mW cm^{-2} gmetal^{-1} and PtRu/C ETEK with the HISPEC cathode achieves 200 mW cm^{-2} gmetal^{-1}. The performance of the functionalized material is at least 78% better compared to the commercial materials. The polarization curve in Fig. 10 reveals improved performance of the electrocatalyst supported on grafted carbon black in the region dominated by ohmic drop. This can be attributed to better proton transfer compared to that in other non-grafted materials. The DMFC polarization curves and power density curves, working with methanol at approx. 1.0 mol L^{-1} (3.5 wt.%) and air, are shown in Fig. 11. The PtRu/C-PSSH electrocatalyst achieves a maximum power density of 70 mW cm^{-2} gmetal^{-1}. The PtRu/C ETEK achieves 35 mW cm^{-2} gmetal^{-1} and the PtRu/C ETEK with the HISPEC cathode achieves 16 mW cm^{-2} gmetal^{-1}. The performance of
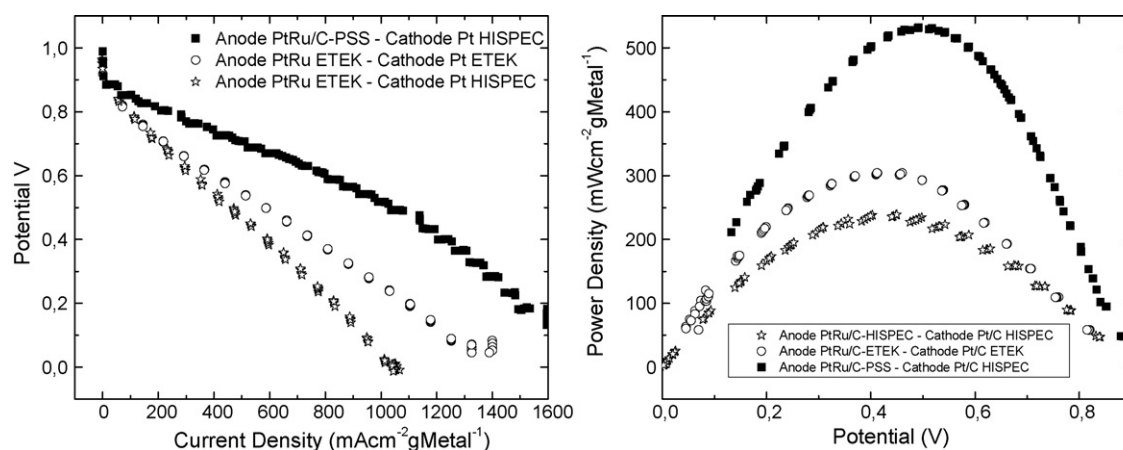

Fig. 10. (a) Polarization curves working with H$_2$/air. Operational conditions: test cell: HIAT FC25/125; cell pressure: 1.0 N mm^{-2}; air: 2.5 NL min^{-1} (100% humidity); H$_2$: 0.8 NL min^{-1} (85% humidity); cell temperature: 70 °C; GDLs: anode toray; cathode SGL 10 CC and (b) power density versus potential curves, working with H$_2$/air, operational conditions: test cell: HIAT FC25/125; cell pressure: 1 N mm^{-2}; air: 2.5 NL min^{-1} (100% humidity); H$_2$: 0.8 NL min^{-1} (85% humidity); cell temperature: 70 °C; GDLs: anode toray, cathode SGL 10 CC.
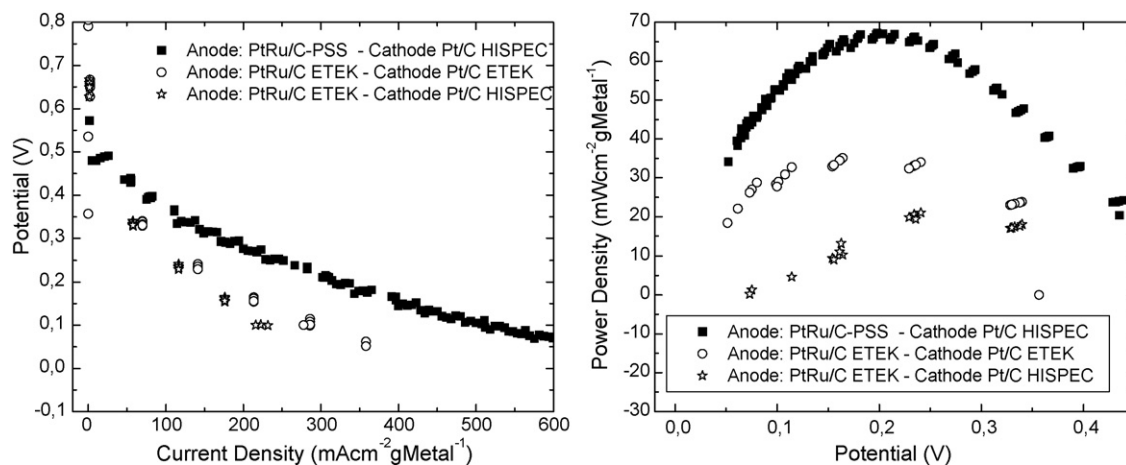

Fig. 11. (a) Polarization curves, working with methanol/air, operational conditions: and the experimental conditions for DMFC were test cell: HIAT FC25/125, cell pressure: 1 N mm^{-2}; air: 1.5 NL min^{-1} (100% humidity); CH$_3$OH 3.5%: 15 mL min^{-1}; cell temperature: 70 °C; GDLs: anode toray, cathode SGL 10 CC. (b) Power density versus potential curves, working with methanol/air, operational conditions: and the experimental conditions for DMFC were test cell: HIAT FC25/125; cell torch: 1 N mm^{-2}; air: 1.5 NL min^{-1} (100% humidity); CH$_3$OH 3.5%: 15 mL min^{-1}; cell temperature: 70 °C; GDLs: anode toray, cathode SGL 10 CC.

the grafted material is at least 100% better compared to the commercial materials. Summarizing, the results present the following performance order: PtRu/C-PSSH > PtRu/C ETEK with ETEK cathode > PtRu/C ETEK with HISPEC cathode.

The chemical stability of the grafted material is an important issue that needs to be addressed and considered. Moreover, if we consider that the presence of the Fluor in the Nafion's structure is a crucial fact for chemical stability, it would be obvious to keep this fact in mind. We have previously studied the prepared materials for a maximum period of 100 h (fuel cell environment) and the material proved to be stable in this period. Long term operation studies, amongst others, for these prepared materials are already planned, and it will be part of future projects.

4. Conclusions

BET results show that the specific surface area of the carbon support after functionalization is reduced by 85%, indicating that the treatment used changes the carbon pore structure markedly. It is suggested that the oxygen surface groups produced by the HNO_3 treatment and the grafted polymeric chains are fixed at the entrance of the micropores, blocking the diffusion of species into the micropores. The TEM images reveal a very homogeneous and uniform particle distribution for the PtRu/C-PSSH material and a less homogeneous distribution for the PtRu/C material. A decrease in the ohmic drop polarization region and/or an increase in proton transfer by the grafted polymeric chains introduced on the carbon black pore structure are observed. This beneficial behavior results in remarkable improved performance, 78%, for PEMFC and 100%, for DMFC, indicating that this might be a promising novel support for fuel cell applications. These results open a new investigation field, the specific functionalization of the carbon/electrolyte or carbon/electrocatalyst surfaces for PEMFC and DMFC applications.

Acknowledgements

References

[1] M. Mastragostino, A. Missiroli, F. Soavi, Journal of the Electrochemical Society 151 (11) (2004) A1919–A1924.
[2] Z.B. Wang, G.P. Yin, P.F. Shi, Carbon 44 (1) (2006) 133–140.
[3] M. Uchida, et al., Journal of the Electrochemical Society 145 (11) (1998) 3708–3713.
[4] V. Rao, et al., Journal of Power Sources 145 (2) (2005) 178–187.
[5] S. Biniak, G. Szymanski, J. Siedlewski, A. Swiatkowski, Carbon 35 (12) (1997) 1799–1810.
[6] B.K. Pradhan, N.K. Sandle, Carbon 37 (8) (1999) 1323–1332.
[7] F. Rodriguezreinoso, et al., Applied Catalysis 15 (2) (1985) 293–300.
[8] F. Rodriguezreinoso, et al., Journal of Catalysis 99 (1) (1986) 171–183.
[9] L. Cao, et al., Chemistry Letters 33 (5) (2004) 490–491.
[10] Y.Q. Liu, A. Adronov, Macromolecules 37 (13) (2004) 4755–4760.
[11] G. Viswanathan, et al., Journal of the American Chemical Society 125 (31) (2003) 9258–9259.
[12] H.S. Liu, et al., Journal of Power Sources 155 (2) (2006) 95–110.
[13] N. Tsubokawa, Journal of Polymer Science Part A: Polymer Chemistry 22 (6) (1984) 1515–1524.
[14] K. Ohkita, N. Tsubokawa, E. Saitoh, Carbon 16 (1) (1978) 41–45.
[15] K. Ohkita, et al., Carbon 13 (5) (1975) 443–448.
[16] K. Ohkita, N. Nakayama, M. Shimomura, Carbon 18 (4) (1980) 277–280.
[17] M. Shimomura, Y. Sanada, K. Ohkita, Carbon 19 (4) (1981) 326–327.
[18] N. Tsubokawa, Journal of Polymer Science Part A-Polymer Chemistry 25 (7) (1987) 1979–1988.
[19] N. Tsubokawa, K. Fujiki, Y. Sone, Journal of Macromolecular Science-Chemistry A25 (9) (1988) 1159–1171.
[20] K. Fujiki, N. Tsubokawa, Y. Sone, Polymer Journal 22 (8) (1990) 661–670.
[21] M. Carmo, J.G.R. Poco, M. Linardi, Process of carbons functionalization by the growth of polymeric chains with ion exchange properties for polymer electrolyte fuel cell applications, Patent - WIPO - World Intellectual Property Organization, Pub. No WO/2008/074113, International Application No.: PCT/BR2007/000354, Publication Date: 26.06.2008.
[22] J. Zawadzki, Chemistry and Physics of Carbon 21 (1989) 147–380.
[23] S. Shin, J. Jang, S.H. Yoon, I. Mochida, Carbon 35 (12) (1997) 1739–1743.
[24] C. Moreno-Castilla, F. Carrasco-Marin, F.J. Maldonado-Hodar, J. Rivera-Utrilla, Carbon 36 (1–2) (1998) 145–151.
[25] M. Starsinic, R.L. Taylor, P.L. Walker, P.C. Painter, Carbon 21 (1) (1983) 69–74.
[26] B.J. Meldrum, C.H. Rochester, Journal of the Chemical Society-Faraday Transactions 86 (21) (1990) 3647–3652.
[27] V. Gomezserrano, M. Acedoramos, A.J. Lopezpeinado, C. Valenzuelacalahorro, Thermochimica Acta 291 (1–2) (1997) 109–115.
[28] I.I. Salame, T.J. Bandosz, Journal of Colloid and Interface Science 210 (2) (1999) 367–374.
[29] J. Barkauskas, M. Dervinyte, Journal of the Serbian Chemical Society 69 (5) (2004) 363–375.
[30] J.P. Chen, S.N. Wu, Langmuir 20 (6) (2004) 2233–2242.
[31] C. Morenocastilla, et al., Langmuir 11 (11) (1995) 4386–4392.
[32] C. Moreno-Castilla, M.V. Lopez-Ramon, F. Carrasco-Marin, Carbon 38 (14) (2000) 1995–2001.
[33] A. Guha, W.J. Lu, T.A. Zawodzinski, D.A. Schiraldi, Carbon 45 (7) (2007) 1506–1517.
[34] F. Scheiba, et al., Journal of Power Sources 177 (2008) 273–280.
[35] M. Carmo, A.R. Dos Santos, J.G.R. Poco, M. Linardi, Journal of Power Sources 173 (2007) 860–866.
[36] M. Carmo, V.A. Paganin, J.M. Rosolen, E.R. Gonzalez, Journal of Power Sources 142 (1–2) (2005) 169–176.